On the "Slow Mode" Mechanism in ENSO-Related Coupled Ocean–Atmosphere Models

CHUNZAI WANG AND ROBERT H. WEISBERG

Department of Marine Science, University of South Florida, St. Petersburg, Florida

(Manuscript received 13 August 1993, in final form 24 March 1994)

ABSTRACT

A linear perturbation, coupled ocean–atmosphere model is revisited for further insights into the El Niño–Southern Oscillation phenomenon. The model oscillates as a slow, eastward propagating mode interpreted as a divergence mode, whose energetics are controlled by the ocean. Growth requires that the work performed by the wind stress minus the work required to effect the ocean divergence exceeds the loss terms. The intrinsic scale of the atmosphere relative to the basin width is important. For sustainable oscillations, the ocean basin must be large enough so that oppositely directed divergence can develop on opposite sides of the basin. The global aspect of the atmospheric pressure field suggests that continental heating may provide either a direct source affecting adjacent oceans, or a connection between oceans. The important model parameters are the coupling and warming coefficients and the ocean Kelvin wave speed. The importance of the Kelvin wave speed derives from its specification of the background buoyancy state for the ocean. Upon further simplification, an analytical solution gives similar parameter dependence as found numerically and shows that growth requires both large zonal wavelength and a zonal phase lag between the anomalies of wind stress and SST.

1. Introduction

Treating the El Niño–Southern Oscillation (ENSO) as a phenomenon of the tropical ocean–atmosphere system has greatly advanced the understanding of interannual climate variability. A broad range of coupled ocean–atmosphere models has been explored over the past decade beginning with the conceptual model of McCreary (1983); the development of the coupling physics by Philander et al. (1984); and the subsequent applications of linear perturbation models, models linearized about different background states, and primitive equation general circulation models (GCM). Mechanistic interpretations of these models have varied, leading to three hypotheses: 1) the delayed oscillator (Suarez and Schopf 1988; Battisti and Hirst 1989), arguing for the importance of equatorial ocean Rossby waves reflected at the western boundary; 2) external heating (Budin and Davey 1990; Masumoto and Yamagata 1991), arguing for the importance of continental heat sources; and 3) the slow thermal or SST mode (Hirst 1986, 1988; Neelin 1991), arguing for the importance of a slowly propagating coupled mode distinctly different from the conventional equatorially trapped waves.

The model ENSOs found in the linearized models of Zebiak and Cane (1987), Battisti (1988), Suarez and Schopf (1988), and Xie et al. (1989) have been attributed to the delayed oscillator mechanism. Wakata and Sarachik (1991) emphasized the importance of spatial variations in the mean thermocline depth and upwelling for determining the evolution of the SST anomalies. The meridional profile of the mean upwelling determines whether the SST anomaly is stationary or eastward propagating, and the delayed oscillator mechanism works only if the mean upwelling is narrowly confined to the equator. This suggests a critical dependence of the delayed oscillator on the ocean background state.

Masumoto and Yamagata (1991) argue that nonlinearities in the Anderson and McCreary (1985a,b) model result in external heating being necessary to sustain coupled oscillations. Without land heating, the coupled system settles into a perpetual El Niño state.

Depending upon the treatment of the ocean thermodynamics in models linearized about a background state, coupled modes may propagate eastward, westward, or remain stationary. Hirst (1986) defined four models, each distinguished by the SST equation. With SST proportional to the thermocline thickness anomaly, the oceanic Kelvin wave is destabilized. With the rate of change of SST proportional to zonal advection and thermal damping, the gravest oceanic Rossby wave is destabilized. By considering thermocline thickness and thermal damping, with or without advection, a slowly propagating unstable mode occurs. Using a perturbation expansion, Neelin (1991) showed that this slow (SST) mode is distinctly different from the conventional equatorial ocean wave modes, leading to the argument that the time delay by ocean wave propagation is not essential to the slow mode.

Corresponding author address: Dr. Robert H. Weisberg, Department of Marine Science, University of South Florida, 140 Seventh Avenue South, St. Petersburg, FL 33701-5016.

Primitive equation GCMs also produce ENSO-like phenomena. Lau et al. (1992) and Philander et al. (1992) discuss results for low- and high-resolution ocean GCMs coupled with an atmospheric GCM, respectively. These models simulate ENSO, but in different ways, and the authors attribute the differences to model resolution.

Given the facts that linear perturbation models, models linearized about differing background states, and GCMs all produce ENSO-like phenomena with different interpretations, the present state of ENSO understanding remains somewhat puzzled. Among the many issues not fully resolved are 1) the mechanism of the slow mode and its relation to the delayed oscillator, 2) the conditions for slow mode growth, 3) the ocean basin size necessary to sustain a slow mode, 4) the importance of continental heating, 5) the importance of the ocean background state, and 6) the importance of the ocean Kelvin wave speed. In view of the complexities in models and interpretations, the present paper considers the simplest of models, namely, a linear perturbation model of the form used by Hirst (1988), to gain insights on these questions. Although the model is overly simple due to homogeneous parameters and lack of background state influences in the thermodynamic equation, it is useful to illustrate possible physical interactions between the ocean and the atmosphere. Section 2 formulates a numerical model and section 3 examines its behavior relative to the above questions. Upon simplification, an analytical solution is obtained in section 4 showing the essential aspects of the model parameters. A discussion and summary then follow in section 5.

2. Formulation of the coupled model

The ocean component is a linear, equatorial β plane, reduced-gravity model forced by surface wind stress. The governing equations are

$$\frac{\partial u}{\partial t} - \beta y v = -g' \frac{\partial h}{\partial x} + \frac{\tau^x}{\rho H_0} - \gamma u, \tag{2.1}$$

$$\frac{\partial v}{\partial t} + \beta y u = -g' \frac{\partial h}{\partial y} + \frac{\tau^y}{\rho H_0} - \gamma v, \tag{2.2}$$

$$\frac{\partial h}{\partial t} + H_0\left(\frac{\partial u}{\partial x} + \frac{\partial v}{\partial y}\right) = -\gamma h, \tag{2.3}$$

where u and v are the velocity components in the zonal (x) and meridional (y) directions, h is the upper-layer thickness perturbation about the mean depth H_0, t is time, g' is the reduced gravity, β is the planetary vorticity gradient, τ^x and τ^y are the zonal and meridional wind stress components, and γ is the coefficient of Rayleigh friction and Newtonian cooling.

Sea surface temperature (SST) is controlled by ocean processes and surface heat fluxes. The simplest formulation for the SST anomaly T is

$$\frac{\partial T}{\partial t} = \sigma h - \alpha T, \tag{2.4}$$

where σh and αT embody the ocean processes and the surface fluxes, respectively, and σ and α are warming and thermal damping coefficients.

The atmosphere component is a steady state, linear, equatorial β plane, reduced-gravity model forced by heating (Gill 1980). The governing equations are

$$a u_a - \beta y v_a = -\frac{\partial p}{\partial x}, \tag{2.5}$$

$$a v_a + \beta y u_a = -\frac{\partial p}{\partial y}, \tag{2.6}$$

$$a p + c_a^2\left(\frac{\partial u_a}{\partial x} + \frac{\partial v_a}{\partial y}\right) = -Q_a, \tag{2.7}$$

where the velocity components and coordinate axis are as defined in the ocean model, p is the pressure anomaly, a is the coefficient of Rayleigh friction and Newtonian cooling, Q_a is the atmospheric heating, and c_a is the reduced-gravity wave speed.

The model ocean is evaluated on a staggered Arakawa C grid with a uniform spacing of 55 km and a time step of 1 h. The ocean model domain is rectangular, extending over 160° of longitude between 20°N and 20°S. The western and eastern boundaries are either rigid or open, and the northern and southern boundaries are open (Camerlengo and O'Brien 1980). Similar to Zebiak (1982), the atmosphere model equations are combined into a second-order ordinary differential equation in y after Fourier transform in x. This is solved numerically and the wind and pressure fields are then obtained by inverse Fourier transform. The atmosphere model domain is rectangular, extending over 360° of longitude between 20°S and 20°N with grid spacings of 440 km and 220 km in x and y, respectively, and the atmosphere is updated daily. The atmosphere model is cyclic in longitude with rigid northern and southern boundaries.

Following Philander et al. (1984) and Hirst (1986), the heat and momentum fluxes are parameterized as

$$Q_a = K_Q T, \tag{2.8}$$

$$\tau/\rho H_0 = (\tau^x, \tau^y)/\rho H_0 = K_S(u_a, v_a), \tag{2.9}$$

where K_Q and K_S are coupling coefficients. This coupled model is thus very similar to the Hirst (1988) model IV, hereafter referred to as H88. Focus will be upon the slow mode mechanism of the model. As a model limitation, it is noted that by omitting a mean zonal thermocline tilt along the equator the model thermodynamics may overestimate the ocean–atmosphere coupling in the west.

3. Numerical results

The model oscillates over a broad range of parameters. This section describes the behavior of the coupled

TABLE 1. Parameters for the standard experiment.

Parameter	Value
H_0	200 m
c	2 m s^{-1}
c_a	60 m s^{-1}
a	(5 days)$^{-1}$
γ	(100 days)$^{-1}$
α	(100 days)$^{-1}$
σ	5.0×10^{-9} K m^{-1} s^{-1}
K_Q	5.0×10^{-3} m^2 s^{-3} K^{-1}
K_S	0.8×10^{-7} s^{-1}
ρ	1.024×10^3 kg m^{-3}
β	2.29×10^{-11} m^{-1} s^{-1}

oscillations, adds to the parameter studies of H88, and offers further mechanistic insights. The experiments begin by perturbing a resting ocean and atmosphere with a positive, Gaussian-shaped SST anomaly located symmetric about the equator in the center of the basin. The coupled model then evolves without modification, using the standard parameters of Table 1.

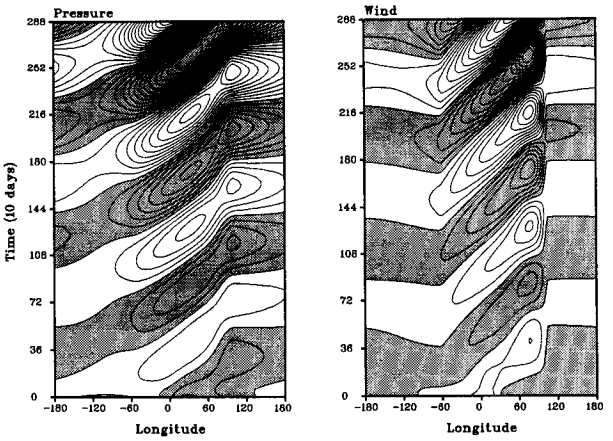

FIG. 2. The evolutions on the equator, as a function of longitude and time, of the coupled model global (a) atmospheric pressure (geopotential height) and (b) zonal wind anomalies. Stippled (clear) regions denote negative (positive) anomalies. The contour intervals for pressure and wind are 10 m^2 s^{-2} and 1.5 m s^{-1}, respectively.

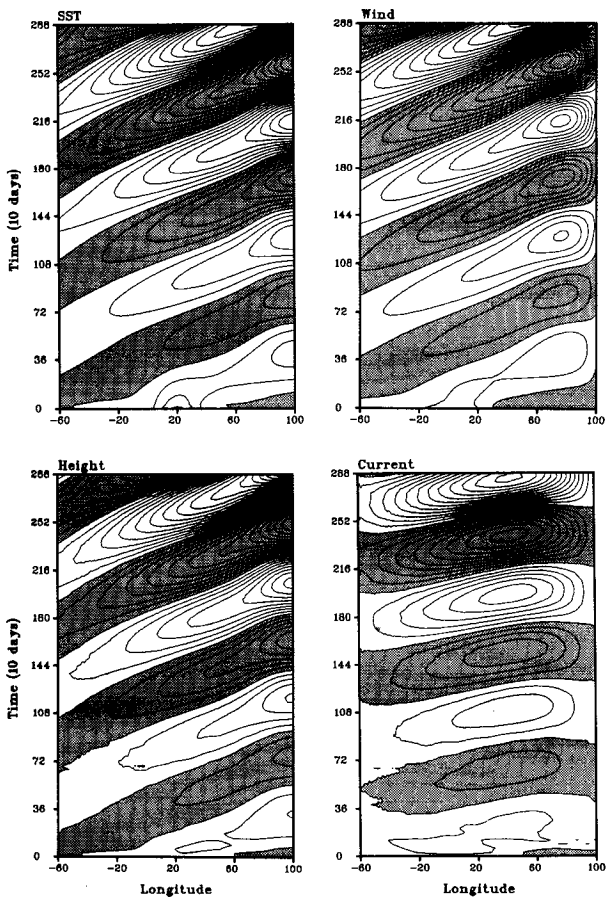

FIG. 1. The evolutions on the equator, as a function of longitude and time, of the coupled model (a) SST, (b) zonal wind, (c) thermocline thickness, and (d) zonal current anomalies. Stippled (clear) regions denote negative (positive) anomalies. The contour intervals for SST, wind, height, and current are 0.6 K, 1.5 m s^{-1}, 20 m, and 0.15 m s^{-1}, respectively.

a. Description of the coupled response

Consistent with Gill (1980), heating symmetric about the equator induces a primarily zonal wind response, with maximum convergence just east of the maximum heating region. The specified model thermodynamics causes an eastward shift in the SST anomaly and hence an eastward translation of the coupled response. The resulting evolutions of the SST, zonal wind, thermocline thickness, and zonal current anomalies on the equator are shown in Figs. 1a, 1b, 1c, and 1d, respectively. For the standard parameters the anomalies oscillate at a periodicity of 2.5 years and grow exponentially as they propagate eastward at a speed of 0.28 m s^{-1} (which is much slower than the ocean Kelvin wave speed of 2.0 m s^{-1}). The SST anomalies lag the thermocline height anomalies and the zonal wind anomalies lag the SST anomalies. These lags result in a zonal phase difference between the SST and zonal wind anomalies at any given time which, as shown in section 4, is important for coupled mode growth. In contrast to the similar zonal phase gradient for the SST, thermocline thickness and zonal wind anomalies, the phase gradient for the zonal current anomalies is smaller and these anomalies are largest in the east central portion of the basin.

The atmosphere response is not limited to the ocean basin domain, as shown in Figs. 2a,b for pressure and zonal wind, respectively. The pressure response is global, with maximum values over the east central Pacific and the South American continent. The wind response (proportional to the zonal pressure gradient) is

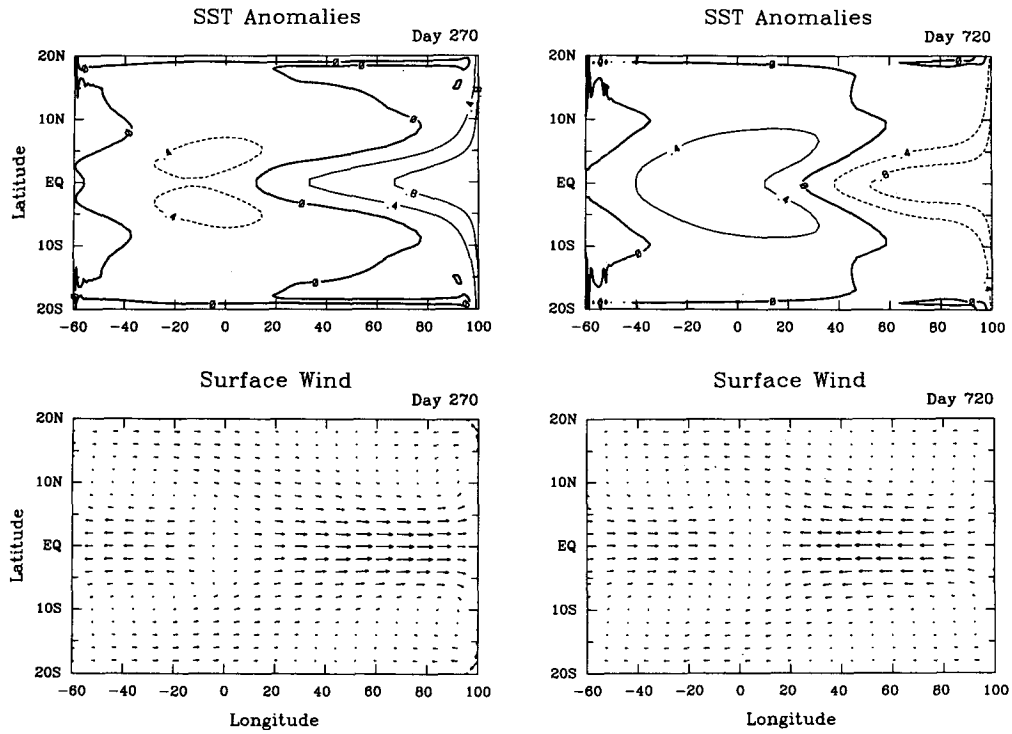

FIG. 3. The horizontal structures of the (a) SST and (b) wind anomalies at day 270; and (c) SST and (d) wind anomalies at day 720. Units are K for SST and m s^{-1} for wind.

large only over the model ocean, since SST provides the only atmosphere heat source. While the lack of continental heating is unrealistic, several important points are noted. First, there is a difference in scale (both zonal and meridional) between the atmosphere and ocean responses. Second, without a continental heat source, the pressure anomaly is blocked by the discontinuity between ocean and land heating. Large zonal pressure gradient and wind anomalies therefore develop near the eastern boundary except when the SST anomaly there goes to zero, at which time the pressure anomaly evolves across the land portion of the cyclic domain and the coupled model oscillates.

SST in this model is forced by ocean divergence [Eqs. (2.3) and (2.4)]. Following the warm anomaly in Fig. 1, it is observed that divergent (convergent) currents occur in the western (eastern) Pacific, resulting in upwelling (downwelling) and SST cooling (warming). The propagating SST anomaly induces a pattern of wind divergence and convergence that supports the eastward propagation. The culmination of the warmest and coldest SST anomalies in the eastern part of the basin may thus be likened to the El Niño and La Niña phases of ENSO. Prior to the first warm phase, the SST and wind anomaly fields for day 270 are shown in Figs. 3a,b. Note the relative positions of the wind divergence and SST anomaly patterns, with the wind divergence pattern centered just to the east of the SST pattern. Strong winds on either side of the wind divergence alters the ocean divergence resulting in eastward propagation. During the mature phase of the model El Niño, the west central Pacific is a region of wind divergence, whereas the eastern Pacific is a region of wind convergence. As the wind pattern continues to move eastward it reverses sign around day 570, resulting in the warming of the western Pacific and the cooling of the eastern Pacific peaking as the cold phase of ENSO around day 810. Prior to this, the SST and wind anomaly fields for day 720 are shown in Figs. 3c,d. Thus, the model ENSO may be summarized as a continuous propagation of ocean divergence and convergence patterns caused by the ocean–atmosphere interaction.

b. Effects of parameters

1) THE PARAMETERS K_Q, K_S, σ, α, AND γ

The Hirst (1988) Model IV explored the sensitivity of the coupled oscillations to K_Q, K_S, σ, and α, where K_Q and K_S set the interactions between the ocean and the atmosphere and σ and α set the relative importance of ocean processes and surface fluxes in determining

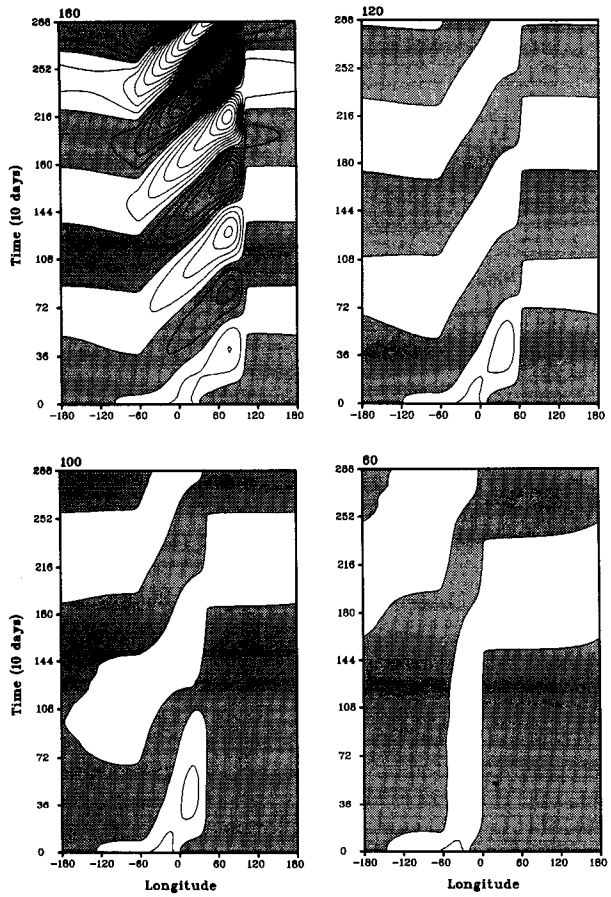

FIG. 4. The global zonal wind anomaly on the equator as a function of longitude and time for bounded ocean basin widths of (a) 160°, (b) 120°, (c) 100°, and (d) 60°. In each case the oceans western boundary is located at −60° longitude. Stippled (clear) regions denote negative (positive) anomalies.

SST. As a test of our model formulation, these studies were repeated with very similar results: the model exhibits evanescent, neutral, or growing modes over a broad range of parameters.

The behavior of the coupled oscillations relative to the parameters follows from the mechanism of the model. For example, in contrast to the H88 finding of increasing frequency with increasing K_Q and K_S, Wakata and Sarachik (1991) found the opposite result. They attributed their model oscillations to the delayed oscillator mechanism, wherein reflected waves interact with directly forced waves reversing the state of upwelling or downwelling. Increasing K_Q and K_S increases the directly forced part of the solution, making it more difficult for the reflected waves to compete. By increasing the time required to change the sign of the ocean divergence, this decreases the frequency. The slow mode mechanism is different. Increasing K_Q and K_S increases the speed at which this mode propagates thereby increasing the frequency.

Varying γ relative to K_Q and K_S shows that growth can occur even for large γ, which also suggests a mechanism different from the delayed oscillator. If the combined effects of the coupling and the efficiency of the ocean processes in effecting SST are large enough then the coupled oscillations can grow despite dissipation. For the other parameters of Table 1, $\gamma = (80 \text{ days})^{-1}$ yields a neutral mode, so for small growth $\gamma = (100 \text{ days})^{-1}$ was chosen for the standard parameter set.

2) THE OCEAN KELVIN WAVE SPEED c

To investigate the effects of varying the ocean Kelvin wave speed, the standard experiment was repeated using $c = 2.4 \text{ m s}^{-1}$, versus 2 m s^{-1}. This resulted in damping, versus growth, and an increase in period. The explanation follows from the change in the background state buoyancy as specified by c. Increasing c, by increasing buoyancy, decreases divergence, since the ratio of thermocline thickness perturbation to current perturbation is $h/u = H_0/c$. Decreasing the ocean divergence decreases the rate of slow mode growth.

In their analysis of the delayed oscillator, Battisti and Hirst (1988) found both the growth rate and period to decrease with decreasing delay time (increasing c). The decrease in period differs from our result due to the different mechanisms of these models. For the delayed oscillator, varying c varies the delay time, while for the slow mode it varies the ocean divergence. Neelin (1991) argued that the timescale for equatorial wave propagation is not essential to the slow mode based upon distorted physics experiments with a GCM. These experiments, however, distorted the effects of wave speed independent of buoyancy. In contrast, the importance of c in our experiment is its effect on buoyancy. This accounts for the sensitivity here, versus the insensitivity in Neelin (1991).

3) THE OCEAN BASIN LENGTH

Experiments were performed with varying ocean widths. Figure 4 shows the zonal wind anomaly on the equator over the global domain for basin widths of 160°, 120°, 100°, and 60°, using the parameters of Table 1. In each case the western boundary is at −60° longitude. Only the 160° case shows growth; modes within the smaller basins decay. The distinguishing feature of the growing mode is the reversal of sign for the zonal wind, with strong, oppositely directed winds on opposite sides of the basin. For the 100° wide basin there is no appreciable oppositely directed anomaly on the western side of the basin, and for the 60° case the anomaly does not change sign at all. Given the scales of the atmosphere relative to the ocean responses, these findings suggest that for an ocean basin to oscillate it

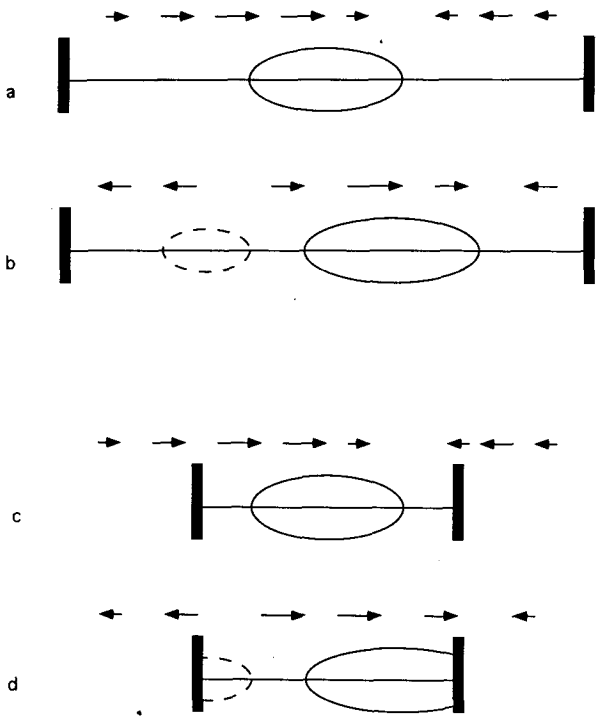

FIG. 5. A schematic on the evolution of the wind responses to initial ocean SST perturbations for large and small ocean basins. (a) and (b) The initial and subsequent stages for the large ocean basin, respectively. (c) and (d) The initial and subsequent stages for the small ocean basin, respectively. For both cases, the initial SST perturbations are the same and are located in the center of the basin as shown. The arrows denote the winds and the dashed line denotes the ensuing SST perturbation of opposite sign.

must be wide enough to contain the atmospheric response, as will be supported by the stability analysis of section 4.

The structure of the wind perturbation issuing from an initial SST anomaly leads to the following hypothesis, as illustrated by Fig. 5. The wind response to the initial ocean heat source consists of a pattern of convergent winds that can promote the growth and propagation of the heat source (e.g., Philander et al. 1984). If the ocean basin is large enough, an SST anomaly of opposite sign can form on the western side due to a developing pattern of divergent winds there while a mature SST anomaly still exists on the eastern side of the basin. Once this occurs, the pattern of convergent and divergent winds, supported by warm and cold SST, may then be self-sustaining. Smaller ocean width makes it more difficult for patterns of opposite sign to evolve. If westward-directed currents are not large enough to promote enough ocean divergence for a given γ, patterns of opposite sign do not form, and the mode decays.

What is large enough is sensitive to the model parameters. Experiments with smaller γ led to oscillations at smaller basin widths, but by the same mechanism (requiring a reversal in the ocean divergence owing to oppositely directed winds). The period of oscillation for smaller γ, however, was several years longer. The smaller basin locked into a nearly steady state until sufficient divergence developed at the western boundary. Once this happened the patterns evolved at a rate similar to the standard case. The oscillations thus appeared as warm and cold states with relatively rapid transitions in between.

c. *Interpretation of the slow mode herein and in H88*

1) FURTHER COMMENTS ON THE DELAYED OSCILLATOR MECHANISM

For the delayed oscillator, westward propagating Rossby waves generated in the central Pacific are reflected at the western boundary as eastward propagating Kelvin waves that tend to change the phase of the warm or cold events. By eliminating the reflected Kelvin waves using an open western boundary, we can determine whether or not this mechanism is operating within the model. The resulting SST anomaly on the equator for the standard parameters is shown in Fig. 6. Compared with Fig. 1a, the evolution of SST is nearly identical for the open or the closed western boundary; the only difference being a small increase in growth rate. Similar behavior between open and closed western boundaries was also found for the smaller γ and smaller ocean basin experiments of the previous section. Therefore, the delayed oscillator is not an important mechanism in this model, regardless of γ or basin size.

Does this finding present an incompatibility between the delayed oscillator and the slow mode paradigms? The same physics are operant in each. Equatorial waves propagate, affecting the depth of the thermocline and the ocean–atmosphere exchanges. For the slow mode these exchanges occur continuously in space and time, whereas the delayed oscillator has a regional dependence, owing to nonhomogeneous parameters. Both directly forced and reflected waves are present for both, but the ocean–atmosphere coupling in the slow mode depends primarily on the directly forced waves. For example, waves directly forced in the western Pacific by strong easterly winds there were important in readjusting the thermocline in the eastern Pacific during the 1982–1983 El Niño termination (e.g., Tang and Weisberg 1984). Where active coupling occurs in nature could therefore determine the relative importance of these two mechanisms without excluding either.

2) INSIGHTS FROM THE ENERGETICS

Following Yamagata (1985) and H88, the equations governing the atmosphere and ocean total perturbation energies, E_a^T and E_o^T, are

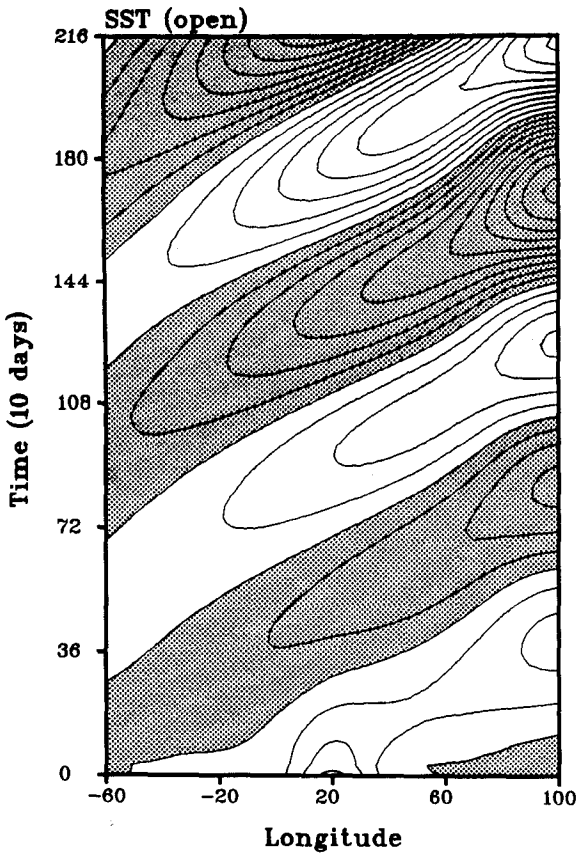

FIG. 6. As in Fig. 1a except with an open western boundary condition.

$$\frac{\partial\langle E_a^T\rangle}{\partial t} = -\frac{\langle pQ_a\rangle}{c_a^2} - \langle \mathbf{u}_a\cdot\nabla p\rangle - \langle p\nabla\cdot\mathbf{u}_a\rangle - \frac{a}{c_a^2}\langle p^2\rangle - a\langle \mathbf{u}_a\cdot\mathbf{u}_a\rangle, \quad (3c.1)$$

$$\frac{\partial\langle E_o^T\rangle}{\partial t} = \frac{1}{\rho H_0}\langle \mathbf{u}\cdot\boldsymbol{\tau}\rangle - g'\langle \mathbf{u}\cdot\nabla h\rangle - g'\langle h\nabla\cdot\mathbf{u}\rangle - \frac{\gamma g'}{H_0}\langle h^2\rangle - \gamma\langle \mathbf{u}\cdot\mathbf{u}\rangle, \quad (3c.2)$$

where E_a^T and E_o^T consist of perturbation kinetic and potential energies [$E_a^T \equiv E_a^K + E_a^P = (u_a^2 + v_a^2)/2 + p^2/2c_a^2$ and $E_o^T \equiv E_o^K + E_o^P = (u^2 + v^2)/2 + g'h^2/2H_0$] and the brackets indicate a model domain average. The first terms on the right-hand sides of these equations are energy sources; the second and third terms represent redistributions between the potential and kinetic energies, which combine to form the pressure work divergence; and the last two terms are potential and kinetic energy dissipation terms.

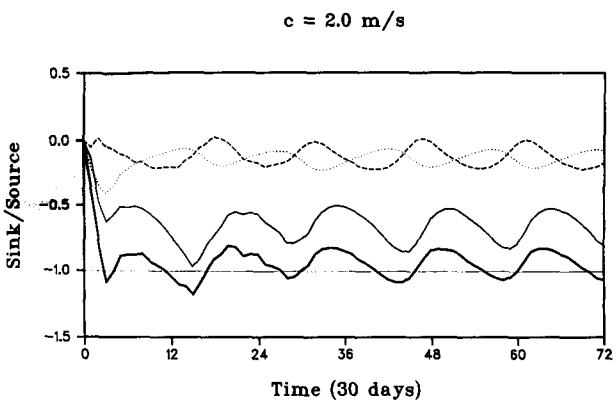

FIG. 7. The ratios of the energy sink terms to the energy source term for the ocean model as a function of time for the standard experiment. The solid, dashed, and dotted lines represent the dissipation of perturbation potential energy, the pressure work divergence, and the dissipation of perturbation kinetic energy, respectively; the bold line is the sum of these three ratios.

An analysis of these equations provides several important points. First, the kinetic energy for the atmosphere is much larger than the potential energy, and conversely for the ocean. It follows that dissipation in the atmosphere (ocean) is mainly due to dissipation of kinetic (potential) energy. Second, the energy source terms $-\langle pQ_a\rangle$, $\langle \tau^x u + \tau^y v\rangle$ are always positive, regardless of whether the coupled model oscillates. This is a consequence of the simple coupling between the reduced-gravity ocean model and the Gill (1980) atmosphere model used herein. It follows that the conditions of positive $-\langle pQ_a\rangle$ and $\langle \tau^x u + \tau^y v\rangle$ are not useful a priori in determining coupled mode growth; they are necessary, but not sufficient, conditions for growth. Third, time series of E_a^T and E_o^T show that the total energy for the atmosphere is smaller than and lags

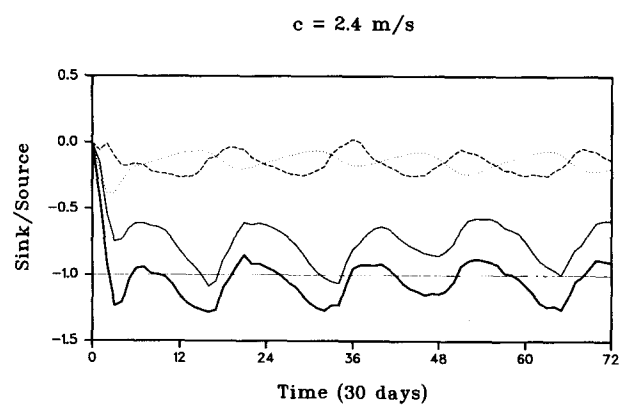

FIG. 8. As in Fig. 7 but with the ocean Kelvin wave speed increased to 2.4 m s^{-1}.

that for the ocean, and that if E_o^T grows so does E_a^T, and conversely. The key to understanding the energetics of the coupled oscillations for this model therefore lies in the ocean energy equation. This is consistent with a conclusion of Barnett et al. (1991), from analyses of uncoupled ocean and atmosphere GCMs, that the propagation of ENSO-related anomalies is determined by the ocean.

The energy equation for the ocean model consists of a source and three sink terms. If the source exceeds the sum of the sinks, the perturbations will grow; if the converse occurs, they will decay. The relative importance of the sink terms for the standard experiment is shown in Fig. 7. Each line represents the ratio of one of the sink terms to the source; the dashed, solid, and dotted lines are the pressure work divergence, the potential energy dissipation, and the kinetic energy dissipation, respectively, and the bold line is their sum. If the sum is greater (less) than -1, the source (sinks) exceeds the sinks (source). The largest sink term is the potential energy dissipation. This is followed by the pressure work divergence (equivalent to an energy transfer to midlatitudes through the open northern and southern boundaries) and the kinetic energy dissipation. The sum of the sink/source ratios in Fig. 7 being greater than -1, on average, is consistent with growth. Figure 8 is a similar presentation for $c = 2.4$ m s^{-1}. Here the sum of the sink/source ratios is less than -1, on average, and the coupled mode decays, as in section 3b.2. The transition from a growing mode to a decaying mode is subtle. All of the terms on the right-hand side of the ocean energy equation grow or decay together, and this is reflected, with a small phase lag, in the growth or decay of the atmosphere energy. The sufficient condition for growth is that the source term for the ocean exceeds the sum of the sinks, but the set of conditions for which this occurs is very sensitive to the parameters. One factor affecting the source term is the difference in phase gradient between the evolution of the winds and currents. Owing to the relative importance of Rossby waves in the ocean current field, the phase gradients for these two quantities are different (Figs. 1c,d), and the larger this difference, the smaller the ocean energy source term.

4. Analytical solution for the slow mode

Noting that the numerically obtained velocity fields for both the ocean and the atmosphere are primarily zonal and analogous to an equatorial Kelvin wave, a solution is sought for the slow mode with v and τ^y both equal to zero. For the model, ocean equations (2.1)–(2.4) become

$$\frac{\partial u}{\partial t} = -g'\frac{\partial h}{\partial x} + \frac{\tau^x}{\rho H_0} - \gamma u, \tag{4.1}$$

$$\beta y u = -g'\frac{\partial h}{\partial y}, \tag{4.2}$$

$$\frac{\partial h}{\partial t} + H_0\frac{\partial u}{\partial x} = -\gamma h, \tag{4.3}$$

$$\frac{\partial T}{\partial t} = \sigma h - \alpha T. \tag{4.4}$$

A closed form solution requires τ^x to be expressed in terms of ocean variables. Battisti and Hirst (1989) found a linear relationship between modeled τ^x and SST anomalies when zonally (and meridionally) averaged over the eastern equatorial Pacific. Our model also shows a correlation between zonally averaged τ^x and SST that is at a maximum on the equator and diminishes to zero poleward of 14°, and a zonal phase difference between τ^x and SST at any given time. We, therefore, assume τ^x to be a linear function of SST lagged by a phase angle θ and seek solutions of the form

$$\begin{pmatrix} u(x,y,t) \\ h(x,y,t) \\ T(x,y,t) \\ \tau^x(x,y,t) \end{pmatrix} = \begin{pmatrix} u(y) \\ h(y) \\ T(y) \\ \rho H_0 \mu T(y) e^{i\theta} \end{pmatrix} e^{i(kx-\omega t)}, \tag{4.5}$$

where μ is a coupling coefficient, k is the zonal wavenumber, the real and imaginary parts of ω are the frequency and the growth rate, respectively, and the other parameters are as in section 2. In view of the decreasing correlation with latitude, the assumption relating τ^x and SST is erroneous, but it does lead to a closed form solution and the error is tempered by the fact that the gravest mode ocean waves are primarily forced by winds near the equator. Substituting Eqs. (4.5) into Eqs. (4.1)–(4.4) yields

$$-i\omega u = -ikg'h + \mu T e^{i\theta} - \gamma u, \tag{4.6}$$

$$\beta y u = -g' h_y, \tag{4.7}$$

$$-i\omega h + ikH_0 u = -\gamma h, \tag{4.8}$$

$$-i\omega T = \sigma h - \alpha T. \tag{4.9}$$

The algebraic equations (4.6), (4.8), and (4.9) have solutions only when

$$\gamma^2 - i2\gamma\omega - \omega^2 + k^2c^2 + \frac{iH_0\mu\sigma k}{\alpha - i\omega}e^{i\theta} = 0. \tag{4.10}$$

This dispersion relationship, cubic in ω, has three roots. It is anticipated that one of these roots should correspond to the Kelvin wave, and one to the slow mode.

First, consider oscillations at frequencies considerably higher than the slow mode. The dispersion relation simplifies to

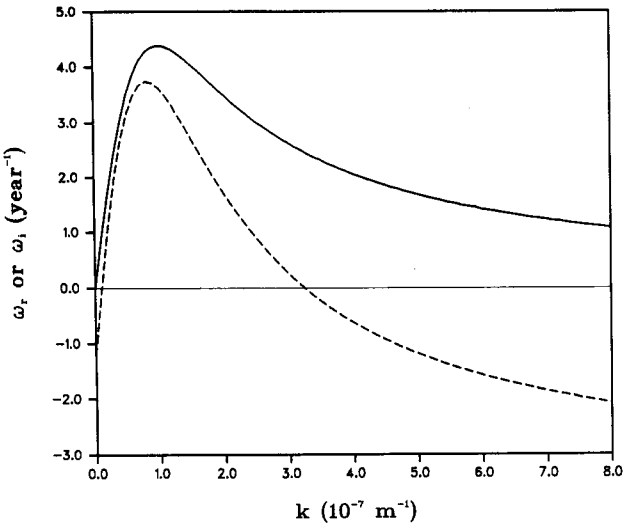

FIG. 9. The real (solid line) and imaginary (dashed line) parts of the analytically derived dispersion relationship for the slow coupled mode. Positive imaginary part denotes growth.

$$\gamma^2 - i2\gamma\omega - \omega^2 + k^2c^2 = 0. \quad (4.11)$$

By writing $\omega = \omega_r + i\omega_i$, we find $\omega_i = -\gamma$ and $\omega_r = \pm kc$. The positive root is the same as a Kelvin wave, damped by ω_i. The negative root is rejected because its associated amplitude increases exponentially with y.

The third root is that of the slow mode. In the low-frequency limit, upon neglecting second- and third-order terms in ω, Eq. (4.10) becomes

$$(\gamma^2 - i2\gamma\omega)\alpha - i\gamma^2\omega + k^2c^2(\alpha - i\omega) + iH_0\mu\sigma k e^{i\theta} = 0, \quad (4.12)$$

which has the solution

$$\omega_r = \frac{H_0\mu\sigma k\cos\theta}{k^2c^2 + \gamma^2 + 2\gamma\alpha}, \quad (4.13)$$

and

$$\omega_i = \frac{H_0\mu\sigma k\sin\theta}{k^2c^2 + \gamma^2 + 2\gamma\alpha} - \frac{\alpha(k^2c^2 + \gamma^2)}{k^2c^2 + \gamma^2 + 2\gamma\alpha}. \quad (4.14)$$

The real part resembles an equatorial Rossby wave dispersion relationship, but with eastward phase propagation. The imaginary part shows that the phase lag between τ^x and SST is necessary for instability. Slow mode growth requires that

$$H_0\mu\sigma k\sin\theta > \alpha(k^2c^2 + \gamma^2), \quad (4.15)$$

which, in turn, requires that $k_1 < k < k_2$, where

$$k_1 = \frac{H_0\mu\sigma\sin\theta}{2\alpha c^2}\left\{1 - \left[1 - \left(\frac{2\gamma\alpha c}{H_0\mu\sigma\sin\theta}\right)^2\right]^{1/2}\right\}, \quad (4.16a)$$

and

$$k_2 = \frac{H_0\mu\sigma\sin\theta}{2\alpha c^2}\left\{1 + \left[1 - \left(\frac{2\gamma\alpha c}{H_0\mu\sigma\sin\theta}\right)^2\right]^{1/2}\right\}. \quad (4.16b)$$

The resulting slow mode dispersion relationship is shown in Fig. 9, using the parameters of Table 1, with $\mu = 1.92 \times 10^{-7}$ m s^{-2} K^{-1} and $\theta = 0.3\pi$. Growth occurs for 0.1×10^{-7} m$^{-1} < k < 3.25 \times 10^{-7}$ m^{-1}, the upper limit of which corresponds to a wavelength of 176°. Wavelengths longer than this value are required for instability.

Given the dispersion relationship, the slow mode eigenfunctions are

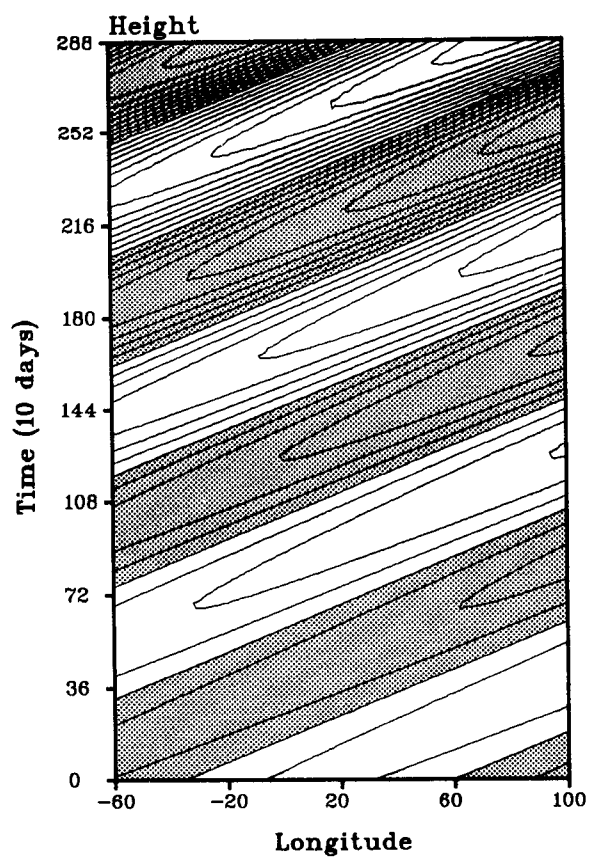

FIG. 10. The thermocline height anomaly on the equator as a function of longitude and time for the analytical solution as given by Eqs. (4.13), (4.14), and (4.17). The parameter values are as given in the text. Note that we have arbitrarily drawn these contours within a 160° wide basin (for comparison with Fig. 1c) without consideration of boundaries.

$$h(x, y, t) = A \exp\left(-\frac{\beta(\omega + i\gamma)}{2kc^2} y^2\right) e^{i(kx-\omega t)}, \quad (4.17)$$

$$u(x, y, t) = \frac{A(\omega + i\gamma)}{kH_0} \times \exp\left(-\frac{\beta(\omega + i\gamma)}{2kc^2} y^2\right) e^{i(kx-\omega t)}, \quad (4.18)$$

$$T(x, y, t) = \frac{A\sigma}{\alpha - i\omega} \exp\left(-\frac{\beta(\omega + i\gamma)}{2kc^2} y^2\right) e^{i(kx-\omega t)}, \quad (4.19)$$

where A is a constant of integration. The meridional scale is $L_s = (\beta\omega_r/kc^2)^{-1/2} = L(c/c_s)^{1/2}$, where $L = (c/\beta)^{1/2}$ is the equatorial radius of deformation and $c_s = \omega_r/k$ is the slow mode phase speed. Since c_s is very much smaller than c, it follows that the meridional scale of the slow mode is larger than the equatorial radius of deformation, consistent with the numerical results of Fig. 3 and the findings of Wang and Weisberg (1994). Using the parameters of Table 1, with $\mu = 1.92 \times 10^{-7}$ m s^{-2} K^{-1}, $\theta = 0.3\pi$, and $k = 3.0 \times 10^{-7}$ m^{-1}, $h(x, 0, t)$ from Eq. (4.17) is shown in Fig. 10. The appearance is very similar to the numerical result of Fig. 1c despite the fact that we have arbitrarily drawn these contours within a 160° wide basin without consideration of boundaries.

The dependencies of ω_r and ω_i on the model parameters are similar to those found numerically. Both ω_r and ω_i increase with increasing coupling and warming coefficients, decrease with increasing Rayleigh friction and thermal damping, and decrease with increasing oceanic Kelvin wave speed. The analytical solution points out the importance of a zonal phase lag between the τ^x and SST anomalies for instability and the narrow range of wavenumbers for which growth occurs.

5. Discussion and summary

Motivated by the state of complexity in ENSO modeling, a model similar to H88 was revisited for insights on the questions raised in section 1. With spatially homogeneous parameters and no background state dependence, other than the reduced-gravity wave speed, the model oscillates as a slow, eastward propagating mode with evanescent, neutral, or growing behavior dependent upon the parameters.

The mechanism of this slow mode differs from that of the delayed oscillator in that ocean waves reflected at the western boundary are not important. With SST governed by [Eqs. (2.3) and (2.4)]

$$\frac{\partial^2 T}{\partial t^2} + (\gamma + \alpha)\frac{\partial T}{\partial t} + \gamma\alpha T = -\sigma H_0\left(\frac{\partial u}{\partial x} + \frac{\partial v}{\partial y}\right), \quad (5.1)$$

which has an evanescent complementary solution, the wind-forced ocean divergence determines the coupled mode growth. For a given τ, the ocean divergence is controlled by the ocean buoyancy (c^2/H_0). Thus, from Eq. (3c.2), if the rate of work by τ minus the rate of work against buoyancy is sufficient to overcome the energy sinks, then the slow mode will grow. With slow propagation speed, the zonal pressure gradient nearly balances τ^x on the equator, so an extremum in thermocline height anomaly coincides approximately with a zero in τ^x. Such an extremum requires that τ^x reverses sign across the ocean basin, consistent with the hypothesis on ocean basin size presented with Fig. 5. The slow mode in this model therefore evolves as a directly forced mode, relatively unaffected by reflected waves.

The results suggest the need for a more global view in ENSO modeling. While the ocean in this model controls the growth and propagation of the slow mode through its divergence field, the atmospheric response is global, due to the atmosphere's large radius of deformation. As the coupled mode evolves, a discontinuity in the atmospheric heat source (proportional to SST) develops at the eastern boundary when the SST anomaly there is large. This effectively blocks the atmospheric pressure anomaly until the SST anomaly goes to zero at the eastern boundary, allowing the atmospheric pressure anomaly to progress cyclically around the global domain. Two important points follow from these pressure variations. First, continental heat sources may be important for transmitting (or blocking) atmospheric pressure perturbations between ocean basins, so adjacent ocean basins may interact if continental heat sources and orographic effects allow for the communication of their pressure perturbations. For example, the out-of-phase behavior observed between the Pacific and Atlantic Oceans during some ENSO events may be a consequence of this. Second, given the large scale of the atmospheric response to a localized heat source, variations in continental heating may initiate a coupled mode within an adjacent ocean basin.

Just how important is the background state in determining coupled oscillations and what is the role of the ocean Kelvin wave speed c? Beginning with the simplest analog model of McCreary (1983) through the more complete GCMs of Lau et al. (1992) and Philander et al. (1992), all models produce oscillations despite the fact that the background states are either neglected or specified to various levels of sophistication. For the linear perturbation model considered herein, slow mode oscillations are robust with respect to the parameters, the most important ones being the coupling and warming coefficients and c. Other than c these coefficients are not well defined: particularly the warming coefficient, a lumped parameter covering all of the ocean processes that give rise to SST variations. To the extent that these ocean processes are modeled incorrectly, thermal damping will provide a correction. This is a major limitation of all coupled models. The

importance of c lies in its specification of the background state buoyancy. Excepting c, the implication is that the background state is important to the extent that the mean conditions control the processes embodied within the warming and coupling coefficients, as in Zebiak and Cane (1987). This remains an issue for future research, including field experimentation to determine the actual role of the various ocean processes, relative to the surface fluxes, in controlling SST.

In summary, the slow mode of a linear perturbation, coupled ocean–atmosphere model with homogeneous coefficients of the form H88 is an ocean divergence mode distinctly different from the delayed oscillator mode. This slow mode propagates eastward. Its energetics are governed by the ocean; the atmosphere merely follows. Growth occurs if the work performed by the wind minus the work required to effect the ocean divergence exceeds the sum of the ocean loss terms. The ocean Kelvin wave speed is therefore an important parameter, since it sets the background buoyancy state of the ocean. For a given level of dissipation the intrinsic length scale of the atmosphere relative to the width of the ocean basin is important. For sustainable oscillations, the ocean basin must be large enough so that oppositely directed divergences can develop on opposite sides of the basin. Analytical results support this with the requirement for sufficiently large wavelength and a zonal phase difference between the τ^x and SST anomalies. The global aspect of the atmospheric pressure component gives importance to both adjacent landmasses and adjacent ocean basins. Continental heat sources may block or facilitate the propagation of the pressure perturbations, or they may provide a direct source affecting an adjacent ocean.

Whether this model has relevance to nature depends upon several factors intrinsic to both the oceans and the adjacent continents. Homogeneous coefficients omit both the background state influences of the ocean circulation and the nonlinear aspects of heat exchange. This facilitates the direct forcing versus the reflected wave behavior of the model which may be unrealistic. Omitting continental heat sources may also be unrealistic. These findings therefore suggest the need for 1) models, incorporating all three oceans and intervening continents; and 2) field experiments, defining the roles of the ocean processes (mean and perturbation) and surface heat fluxes in determining the evolution of SST.

Acknowledgments. Support was provided by the Division of Ocean Sciences, National Science Foundation, Grant Number OCE-9100024. We gratefully acknowledge the discussions with Dr. M. Luther on numerical model development and the constructive criticisms by Dr. J. McCreary and two anonymous reviewers.

REFERENCES

Anderson, D. L. T., and J. P. McCreary, 1985a: Slowly propagating disturbances in a coupled ocean–atmosphere model. *J. Atmos. Sci.*, **42,** 615–629.

——, and ——, 1985b: On the role of the Indian Ocean in a coupled ocean–atmosphere model of El Niño and the Southern Oscillation. *J. Atmos. Sci.*, **42,** 2439–2442.

Barnett, T. P., M. Latif, E. Kirk, and E. Roeckner, 1991: On ENSO physics. *J. Climate,* **4,** 487–515.

Battisti, D. S., 1988: The dynamics and thermodynamics of a warming event in a coupled tropical atmosphere–ocean model. *J. Atmos. Sci.*, **45,** 2889–2919.

——, and A. C. Hirst, 1989: Interannual variability in the tropical atmosphere–ocean model: Influence of the basic state, ocean geometry and nonlinearity. *J. Atmos. Sci.*, **45,** 1687–1712.

Budin, G. R., and M. K. Davey, 1990: Intermediate models of interseasonal and interannual waves in the Tropics. *J. Mar. Sys.*, **1,** 39–50.

Camerlengo, A. L., and J. J. O'Brien, 1980: Open boundary condition in rotating fluids. *J. Comput. Phys.*, **35,** 12–35.

Gill, A. E., 1980: Some simple solutions for heat-induced tropical circulation. *Quart. J. Roy. Meteor. Soc.*, **106,** 447–462.

Hirst, A. C., 1986: Unstable and damped equatorial modes in simple coupled ocean–atmosphere models. *J. Atmos. Sci.*, **43,** 606–630.

——, 1988: Slow instabilities in tropical ocean basin–global atmosphere models. *J. Atmos. Sci.*, **45,** 830–852.

Lau, N. C., S. G. H. Philander, and M. J. Nath, 1992: Simulation of ENSO-like phenomena with a low-resolution coupled GCM of the global ocean and atmosphere. *J. Climate,* **5,** 284–307.

Masumoto, Y., and T. Yamagata, 1991: On the origin of a model warm ENSO in the western Pacific. *J. Meteor. Soc. Japan,* **66,** 197–207.

McCreary, J. P., 1983: A model of tropical ocean–atmosphere interaction. *Mon. Wea. Rev.*, **111,** 370–387.

Neelin, J. D., 1991: The slow sea surface temperature mode and the fast-wave limit: Analytic theory for tropical interannual oscillations and experiments in a hybrid coupled model. *J. Atmos. Sci.*, **48,** 584–606.

Philander, S. G. H., T. Yamagata, and R. C. Pacanowski, 1984: Unstable air–sea interactions in the Tropics. *J. Atmos. Sci.*, **41,** 604–613.

——, R. C. Pacanowski, N. C. Lau, and M. J. Nath, 1992: Simulation of the ENSO with a global atmospheric GCM coupled to a high-resolution, tropical Pacific Ocean GCM. *J. Climate,* **5,** 308–329.

Suarez, M. J., and P. S. Schopf, 1988: A delayed action oscillator for ENSO. *J. Atmos. Sci.*, **45,** 3283–3287.

Tang, T. Y., and R. H. Weisberg, 1984: On the equatorial Pacific response to the 1982/1983 El Niño–Southern Oscillation event. *J. Mar. Res.*, **42,** 809–829.

Wakata, Y., and E. S. Sarachik, 1991: Unstable coupled atmosphere–ocean modes in the presence of a spatially varying basic state. *J. Atmos. Sci.*, **48,** 2060–2077.

Wang, C., and R. H. Weisberg, 1994: Equatorially trapped waves of a coupled ocean–atmosphere system. *J. Phys. Oceanogr.*, **24,** 1978–1998.

Xie, S. P., A. Kubokawa, and K. Hanawa, 1989: Oscillations with two feedback processes in a coupled ocean–atmosphere model. *J. Climate,* **2,** 946–964.

Yamagata, T., 1985: Stability of a simple air–sea coupled model in the Tropics. *Coupled Ocean–Atmosphere Models,* J. C. J. Nihoul, Ed., Vol. 40, Elsevier Oceanography Series, Elsevier, 637–657.

Zebiak, S. E., 1982: A simple atmospheric model of relevance to El Niño. *J. Atmos. Sci.*, **39,** 2017–2027.

——, and M. A. Cane, 1987: A model El Niño–Southern Oscillation. *Mon. Wea. Rev.*, **115,** 2262–2278.